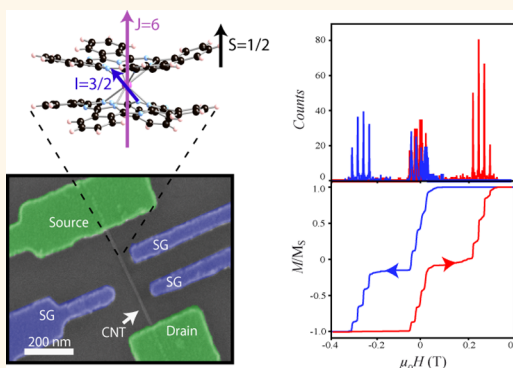


# Magnetic Interaction Between a Radical Spin and a Single-Molecule Magnet in a Molecular Spin-Valve

Matias Urdampilleta,<sup>\*,†,‡</sup> Svetlana Klayatskaya,<sup>‡</sup> Mario Ruben,<sup>\*,†</sup> and Wolfgang Wernsdorfer<sup>\*,†</sup>

<sup>†</sup>Institut Néel-CNRS-UJF-INPG, UPR2940 25 rue des Martyrs BP 166, 38042 Grenoble cedex 9, France, <sup>‡</sup>Institute of Nanotechnology (INT), Karlsruhe Institute of Technology (KIT), 76344 Eggenstein-Leopoldshafen, Germany, and <sup>§</sup>Institut de Physique et Chimie des Matériaux de Strasbourg (IPCMS), CNRS-Université de Strasbourg, 67034 Strasbourg, France <sup>||</sup>Present address: London Center for Nanotechnology, University College London, London WC1H 0AH, United Kingdom.

**ABSTRACT** Molecular spintronics using single molecule magnets (SMMs) is a fast growing field of nanoscience that proposes to manipulate the magnetic and quantum information stored in these molecules. Herein we report evidence of a strong magnetic coupling between a metallic ion and a radical spin in one of the most extensively studied SMMs: the bis(phthalocyaninato)terbium(III) complex (TbPC<sub>2</sub>). For that we use an original multiterminal device comprising a carbon nanotube laterally coupled to the SMMs. The current through the device, sensitive to magnetic interactions, is used to probe the magnetization of a single Tb ion. Combining this electronic read-out with the transverse field technique has allowed us to measure the interaction between the terbium ion, its nuclear spin, and a single electron located on the phthalocyanine ligands. We show that the coupling between the Tb and this radical is strong enough to give extra resonances in the hysteresis loop that are not observed in the anionic form of the complex. The experimental results are then modeled by diagonalization of a three-spins Hamiltonian. This strong coupling offers perspectives for implementing nuclear and electron spin resonance techniques to perform basic quantum operations in TbPC<sub>2</sub>.



**KEYWORDS:** spin–spin interaction · single-molecule magnets · molecular electronic · spintronic · molecular spin-valve

Molecular spintronics is interesting for its hybrid character, at the crossroads between spintronics, molecular electronics, and molecular magnetism.<sup>1</sup> In this new field, one tries to exploit the properties of molecules in order to create original features, useful in spintronics and quantum information.<sup>2</sup> In particular, organic semiconductors are promising since they may offer the possibility of transferring spin information on longer distance and time scale than conventional materials.<sup>3,4</sup> Moreover, molecular material could bring additional functionalities to devices, enabling the control of spin information with different stimuli (e.g., switchability with light,<sup>5</sup> electric field,<sup>6</sup> etc.).

Among the molecular systems, single-molecule magnets (SMMs) have been extensively studied since they behave like quantum magnets<sup>7</sup> and are promising candidates for quantum information processing.<sup>8</sup> On the one hand, they present

magnet-like properties such as a large spin in the ground state along with a large and well-defined magnetic anisotropy. On the other hand, their small dimension grants them quantum properties such as quantum tunneling of magnetization (QTM)<sup>9</sup> and interference effects between tunneling paths.<sup>10</sup> Besides, the synthetic chemistry can produce various SMM structures at high yield and low cost,<sup>11</sup> with functionalizing groups that help grafting SMMs on different supports.<sup>12</sup>

One of the most promising SMMs for magnetic storage and quantum computation is the bis(phthalocyaninato) Tb(III) complex, or TbPC<sub>2</sub>, in the following, depicted in Figure 1. It is a single ion complex,<sup>13</sup> which has the advantage of being magnetically more stable, with regard to mechanical deformations, than other SMMs. The magnetic characterization of the anionic form of TbPC<sub>2</sub> diluted in a diamagnetic matrix of YPC<sub>2</sub> has revealed the importance of nuclear

\* Address correspondence to m.urdampilleta@ucl.ac.uk, wolfgang.wernsdorfer@neel.cnrs.fr.

Received for review February 14, 2015 and accepted April 10, 2015.

Published online April 10, 2015  
10.1021/acsnano.5b01056

© 2015 American Chemical Society

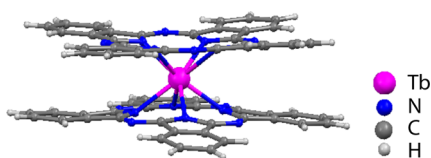


**Figure 1.** Bis(phthalocyaninato) Tb(III) complex. Two phthalocyanine groups coordinate a Tb ion in a  $D_{4h}$  symmetry.

spin driven transitions in the terbium ion.<sup>14</sup> Recently, the quantum properties of this nuclear spin coupled to the Tb ion has been exploited to demonstrate the first coherent manipulation of an isolated SMM spin.<sup>15</sup> As a result and in order to integrate TbPc<sub>2</sub> in electronic devices, it has been extensively studied under different forms: crystal,<sup>14</sup> thin film,<sup>16</sup> or isolated on substrate<sup>17</sup> or between electrodes.<sup>18</sup> In addition, the structure of TbPc<sub>2</sub> can be modified by the adjunction of ligands that would improve the grafting to a particular surface. For instance, the hexyl 6-pyrene substituted TbPc<sub>2</sub>, used in the present article and labeled TbPc<sub>2</sub><sup>\*</sup> in the following, is known to graft with a very good selectivity onto sp<sup>2</sup>-type carbon materials such as graphene<sup>19</sup> or carbon nanotubes.<sup>20</sup>

The neutral form of TbPc<sub>2</sub> has the particularity to have an unpaired electron (radical) delocalized over the two phthalocyanine (Pc) ligands.<sup>21</sup> As a result, this complex forms a three-spins system: the Tb nuclear spin, the Tb electronic moment, and the Pc radical spin. Only coherent manipulations of the nuclear spin have been achieved so far<sup>15</sup> since the terbium electronic moment is EPR-inactive, preventing its manipulation with microwave excitations. Therefore, the coupling between the nuclear spin and the radical through the Tb electronic moment may be of strong interest for quantum information processing, by allowing entanglement between these spins using EPR-NMR sequences.<sup>22</sup> It could also be used to couple together a few nuclear spins in a polynuclear complex such as the tri(phthalocyaninato)Tb<sub>2</sub> complex.<sup>23</sup>

The presence of this unpaired electron located in the Pc has been experimentally demonstrated by tunneling spectroscopy on isolated TbPc<sub>2</sub> deposited on gold substrate.<sup>24</sup> However, the coupling strength between the terbium magnetic moment and the radical has not been measured yet at very low temperature. We propose here to study this coupling in a single neutral isolated TbPc<sub>2</sub><sup>\*</sup> grafted on the surface of a carbon nanotube. The interaction between the Tb complex and the carbon nanotube creates a molecular spin-valve that will be used to read out the magnetic properties of the Tb ion. We will demonstrate how the coupling with the nuclear spin and the radical spin located in the Pc affects its magnetic behavior.

## RESULTS AND DISCUSSION

**Magnetic Properties of TbPc<sub>2</sub>.** In this section, we will first discuss the magnetic properties of the anionic form of

TbPc<sub>2</sub> (with no radical spin on the Pc). The +III oxidation state and the strong spin-orbit coupling in Tb give rise to a total angular momentum of  $J = 6$  in the ground state.<sup>25</sup> The influence of the phthalocyanine groups lifts the degeneracy among the  $J_z$  substates.<sup>26</sup> By using the ligand field parameters of ref 26 and the Stevens operators formalism, we calculate the ground state as a function of the longitudinal magnetic field. The corresponding ligand field and Zeeman Hamiltonians are the following:

$$\mathcal{H}_{\text{lf}} = \alpha A_2^0 O_2^0 + \beta (A_4^0 O_4^0 + A_4^4 O_4^4) + \gamma A_6^0 O_6^0 \quad (1)$$

$$\mathcal{H}_{\text{Zeeman}} = g_J \mu_0 \mu_B \mathbf{J} \cdot \mathbf{H} \quad (2)$$

where the  $O_q^k$  are the Stevens operators,  $A_q^k$  the ligand field parameters,  $\alpha$ ,  $\beta$ , and  $\gamma$  the Stevens constants,  $g_J$  the gyromagnetic factor in Tb, and  $H_z$  the magnetic field applied along the quantization axis. The numerical diagonalization of  $\mathcal{H}_{\text{Zeeman}} + \mathcal{H}_{\text{lf}}$  gives  $J_z = \pm 6$  as a ground doublet, isolated from the first excited state,  $J_z = \pm 5$ , by 600 K. Therefore, we can consider the electronic moment as an Ising-like spin within the low-temperature regime. The presence of a transverse anisotropy,  $A_4^4 O_4^4$  couples the two states  $J_z = \pm 6$  giving rise to an avoided level crossing at the intersection between those states. The amplitude of the tunnel coupling is about 1  $\mu\text{K}$ .<sup>14</sup> As a result, quantum tunneling of the magnetization (QTM) occurs in such molecule when the magnetic field is swept adiabatically through this anticrossing.<sup>27</sup> In the case of a nonadiabatic evolution, the electronic moment ends up in the excited state and can relax to the ground state by emitting a phonon whose energy matches the Zeeman energy. This mechanism is called a direct transition and implies a strong coupling between the electronic moment and the phonon bath. The two mechanisms of magnetization reversal are depicted in Figure 2a and illustrated with a magnetization curve measured by the micro-SQUID technique,<sup>28</sup> on a single crystal of [TbPc<sub>2</sub>]<sup>-</sup> TBA<sup>+</sup> (TBA = tetrabutylammonium) diluted in the diamagnetic [YPC<sub>2</sub>]<sup>-</sup> TBA<sup>+</sup>, see Figure 2b. A large amount of molecules reverses their magnetization by QTM since the total magnetization  $M$  abruptly changes at zero magnetic field, where  $J_z = \pm 6$  are brought into resonance. The remaining molecules, that are in the excited state, continuously reverse their electronic moment at higher magnetic field, using the direct transition mechanism.

We now investigate the magnetic properties of the neutral form. Magnetometry of the neutral TbPc<sub>2</sub> diluted in YPC<sub>2</sub> has been achieved on a single crystal in the same conditions as the anionic form. The magnetization curve of Tb<sub>0.02</sub>Y<sub>0.98</sub>Pc<sub>2</sub> is plotted Figure 2c. For each field sweep direction two steps in the magnetization are visible, one at zero field and one around 70 mT. As sketched in Figure 2d, the compound

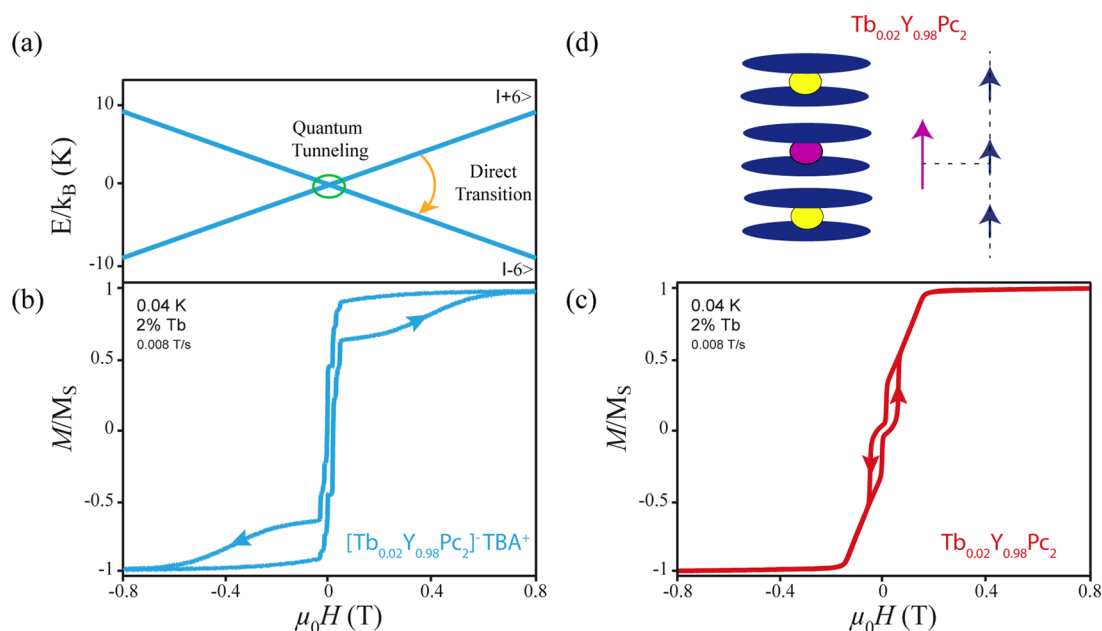


**Figure 2.** (a) Zeeman diagram of the ground electronic doublet in Tb. Quantum tunnelling of the magnetization (QTM) occurs at the intersection between the states  $|J_z = \pm 6\rangle$ . A second mechanism occurs at higher magnetic field, enabling the relaxation from the excited state to the ground state by emission of a phonon. (b) Magnetization curve at 40 mK measured with the micro-SQUID technique on a single crystal made of 2% of  $[\text{TbPc}_2]^- \text{TBA}^+$  diluted in  $[\text{YPc}_2]^- \text{TBA}^+$ . Steps around zero magnetic field are attributed to QTM and the continuous reversal at higher magnetic field to direct transition. (c) Magnetization curve of a  $\text{Tb}_{0.02}\text{Y}_{0.98}\text{Pc}_2$  single crystal. When the magnetic field is swept from negative to positive value, two steps are visible, the first one occurs at zero magnetic field and the second one at 70 mT. (d) Magnetic structure of the neutral form of  $\text{TbPc}_2$  diluted in  $\text{YPc}_2$  crystal. The Pc ligands are sketched in blue color, the Y atom in yellow, and the Tb atom in purple.  $\text{Tb}_{0.02}\text{Y}_{0.98}\text{Pc}_2$  forms a 3D arrangement of spin 1/2 (blue arrows) interacting together. The Tb ion (purple arrow) is locally coupled to a single electron located in the Pc.

is expected to form a 3D network of interacting spins  $S = 1/2$  due to the radical nature of the Pc. Indeed, the magnetic characterization of a pure  $\text{YPc}_2$  crystal has shown a radical–radical interaction of 1 K.<sup>29</sup> One possible interpretation of the magnetization curve is that the transition at zero magnetic field corresponds to the concomitant spin reversal of the Tb ion and the unpaired electron while the transition at finite magnetic field corresponds to the QTM of the Tb ion only followed by a direct transition of the unpaired electron. However, no signature of the hyperfine interaction is visible in contrast with Figure 2b to confirm our assumption. In order to investigate in more detail the interaction occurring in this molecule, we propose in the following to study the magnetization properties of a single neutral  $\text{TbPc}_2^*$  complex thanks to our original carbon-nanotube based detector.

**Molecular Spin-Valve.** The device we use in the present study is made out of a carbon nanotube in a transistor configuration, see Figure 3a. The current is injected and measured thanks to the source and drain electrodes. The side gates are used to control the electric field along the nanotube in order to optimize the detector response. As demonstrated in previous research papers,<sup>30–32</sup> in the case where two molecules are strongly coupled to the nanotube (see Figure 3b), the device behaves as a spin-valve analogue (see Figure 3c). One of the molecule plays the role of a spin polarizer,

while the second one analyzes the spin current. Exploiting this effect allows a complete study of the Tb magnetic moment such as a characterization of its anisotropy,<sup>30</sup> of the Landau–Zener tunnelling, or of the hyperfine interaction.<sup>32</sup> Figure 3d shows the differential conductance as a function of the increasing magnetic field with a  $20 \text{ mT} \cdot \text{s}^{-1}$  sweep rate. Those curves present two abrupt conductance changes related to the magnetization reversal of two molecules coupled to the nanotube. Two different behaviors can be observed in this figure, the green curves present both reversals close to zero field, whereas the orange curves show one reversal close to zero field and a second one above 0.2 T. In the first case, both molecules experience QTM at low field, while in the second case one of the two molecules does not reverse by QTM at low field. This behavior is fully consistent with the stochastic nature of QTM. From the occurrence of QTM events, we can estimate the Landau–Zener probability of tunneling of one molecule to be  $\sim 0.2$ , very close to the theoretical value of 0.25, considering a tunnel splitting of  $1 \mu\text{K}$ . In the case both molecules experience QTM at low field, it is not possible to discriminate which one tunnels first and which conductance jump corresponds to which molecule. To solve this problem we use the transverse field technique,<sup>32</sup> which applies a constant magnetic field perpendicular to the easy axis of the first molecule.

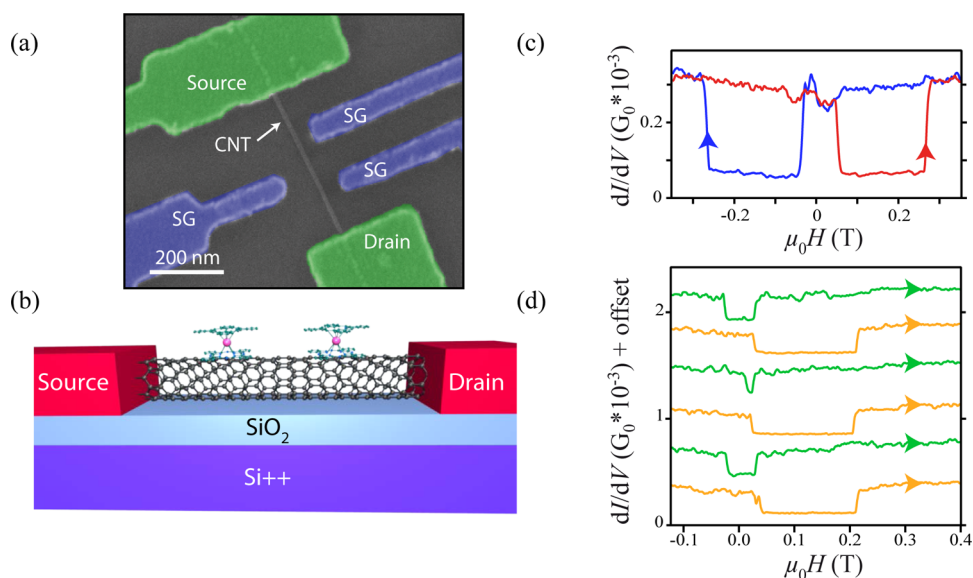


**Figure 3.** (a) SEM micrograph of the sample. Green electrodes correspond to the source and drain and are used to send and measure current through the nanotube (CNT). The blue electrodes are used as side gates to control the electric field and the current through the CNT. (b) Artistic view of the device. The nanotube lies on a SiO<sub>2</sub> substrate supported by a metallic back-gate used to tune the chemical potential of the nanotube. Two molecules are coupled to the nanotube, polarizing and analyzing the electronic current through the nanotube. (c) Spin-valve features observed in the hybrid device composed of a nanotube and two TbPc<sub>2</sub><sup>+</sup> complexes. The red curve is the differential conductance recorded as a function of the magnetic field going from negative to positive value (trace), and the blue curve is recorded for magnetic field going from positive to negative (retrace). Each conductance change is attributed to the magnetic moment reversal of one of the molecules. (d) Trace measurements recorded at 20 mT·s<sup>-1</sup>.

As a result, the transverse field shifts the QTM position of the second molecule, which is misaligned, and allows us to unambiguously study the QTM position of the first molecule.

**Analysis of Spin Reversals.** To analyze the electronic moment reversal of one of the molecules, we apply a constant transverse field of 0.5 T, while the longitudinal field is swept and we store the exact position of the corresponding conductance changes in a histogram. Figure 4a presents the result of 2500 traces in red, i.e., magnetic field going from  $-0.4$  to  $+0.4$  T and the same number of retraces in blue, i.e., magnetic field going from  $+0.4$  to  $-0.4$  T. Three sets of four peaks emerge from the statistics. One is centered around zero field and is present in both trace and retrace. Another appears only in the trace at 0.25 T, mirrored by another set of peaks in the retrace at  $-0.25$  T. To compare with the single crystal hysteresis loop of the anionic form, we integrate the histogram and report the normalized hysteresis loop for a single TbPc<sub>2</sub><sup>+</sup> in Figure 4b. The four steps around zero magnetic field are visible on both hysteresis loops (Figures 2b and 4b) and are attributed to the strong hyperfine coupling between the  $J = 6$  electronic moment and the  $I = 3/2$  nuclear spin in Tb. To take into account this interaction we use the following Hamiltonian:

$$\mathcal{H}_{\text{Tb}} = \mathcal{H}_{\text{hf}} + \mathcal{H}_{\text{Zeeman}} + A\mathbf{I} \cdot \mathbf{J} + P \left( I_z^2 - \frac{1}{3}(\mathbf{I} + \mathbf{1})(\mathbf{I} + \mathbf{1}) \right) \quad (3)$$

where  $J$  and  $I$  are, respectively, the Tb electronic moment and nuclear spin,  $A$  the hyperfine constant, and  $P$  the quadrupolar term. The hyperfine interaction splits the electronic ground doublet  $|J_z = \pm 6\rangle$  in an octuplet  $|J_z = \pm 6, I_z\rangle$  with  $I_z = +3/2, +1/2, -1/2, \text{ or } -3/2$ . Among the 16 intersections within the ground octuplet, only four are avoided level crossing: the ones conserving the nuclear spin state.<sup>18</sup> As a consequence, the four peaks/steps around zero-field in Figure 4a,b correspond to QTMs at these particular anticrossings, which reverse the electronic moment but conserve the nuclear spin.

The transitions appearing at higher magnetic field cannot be explained neither with this model nor with a direct transition picture. In order to study these high field transitions, we increase the sweep rate to reach a regime where only reversal at high magnetic field can be observed. Figure 5a shows the spin-valve features we observe in this regime, at 50 mT·s<sup>-1</sup>, similar to the orange curves in Figure 3d. By contrast with the previous measurement, the hyperfine structure is only visible at high field. We measure the conductance as a function of the longitudinal magnetic field, back and forth, while the transverse field is incremented. The position of reversal is reported on the 2D plot  $(H_{\parallel}, H_{\perp})$ , and then we increment the transverse field by 0.1 mT. Figure 5b presents the evolution of the high field transitions as a function of the transverse field amplitude.

**Interpretation of the Magnetic Interactions.** The position of the high field transitions moves toward higher

longitudinal field when the transverse field is increased. As a consequence, these transitions cannot

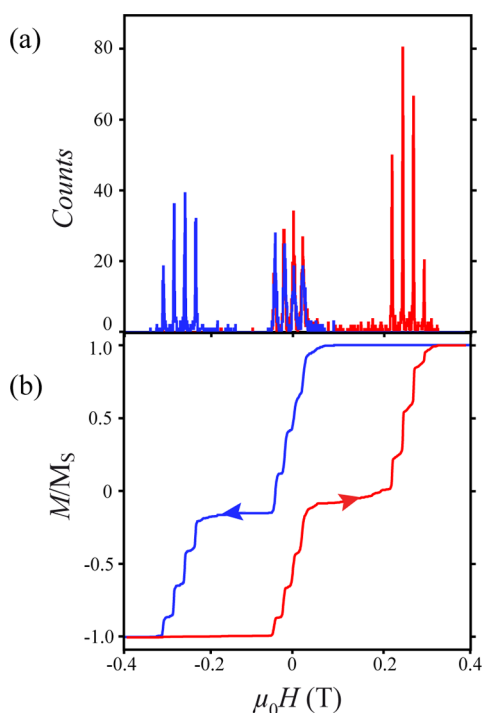


**Figure 4.** (a) Histogram of the magnetization reversal events of a single  $\text{TbPc}_2^*$  complex obtained for 2500 field sweeps at  $20 \text{ mT} \cdot \text{s}^{-1}$  and under a constant 0.5 T transverse field. Each trace (red) and retrace (blue) histogram shows two series of four peaks, one around zero magnetic field and a second one at higher value. (b) Hysteresis loop of a single  $\text{TbPc}_2^*$  complex.

be interpreted in terms of phonon assisted relaxation since the phonon bath or vibron energies are insensitive to magnetic field.<sup>33</sup> We can also exclude any intersection with the higher excited state since the latter is expected to lay at 600 K above the ground state, as calculated in the first section, *vide supra*. As a result, the transverse field evolution implies that the Tb ion couples with another spin system that may be the radical located in the Pc. In order to verify this assumption, we use the following Hamiltonian:

$$\mathcal{H}_{\text{Tb-Pc}} = \mathcal{H}_{\text{Tb}} + \mu_{\text{B}}\mu_0(g_{\text{J}}\mathbf{J} + g_{\text{S}}\mathbf{S}) \cdot \mathbf{H} + \gamma\mathbf{S} \cdot \mathbf{J} \quad (4)$$

where  $\mathbf{J}$  and  $\mathbf{S}$  are, respectively, the Tb electronic moment and the Pc electron spin,  $g_{\text{J}}$  and  $g_{\text{S}}$  the corresponding gyromagnetic factors, and  $\gamma$  the interaction constant between the Tb electronic moment and the Pc radical. The latter is the only fitting parameter in the Hamiltonian. By diagonalizing  $\mathcal{H}_{\text{Tb-Pc}}$  for a constant 0.5 T transverse field and an interaction of 0.4 K, we obtain the Zeeman diagram in Figure 5c. Both sets of peaks in Figure 5d, obtained at low sweep rate  $20 \text{ mT} \cdot \text{s}^{-1}$ , are in agreement with the avoided level-crossings of this diagram. We conclude that the first set is the signature of QTM between the states  $|J_z = +6, I_z, S_z = -1/2\rangle$  and  $|J_z = -6, I^z, S_z = +1/2\rangle$  and the second set of QTM between the states  $|J_z = +6, I^z, S_z = -1/2\rangle$  and  $|J_z = -6, I^z, S_z = -1/2\rangle$  followed by the relaxation to a ground state  $|J_z = -6, I^z, S_z = +1/2\rangle$ .

The assumption of a radical interacting with the Tb ion is supported by combining experiment and simulation with a single fitting parameter: the interaction

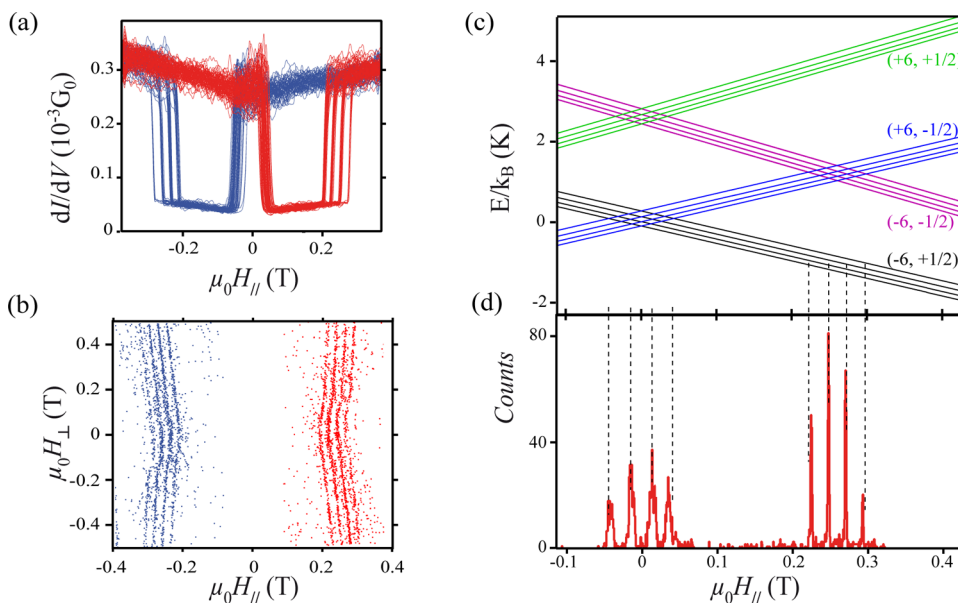


**Figure 5.** (a) Spin-valve feature at  $50 \text{ mT} \cdot \text{s}^{-1}$ , exhibiting resonant transitions at high magnetic field. (b) Evolution of transitions at high magnetic field as a function of the transverse field. Each dot corresponds to a measurement of a magnetization reversal for a constant transverse field with red dots for traces and blue dots for retraces. For clarity, the transitions of the second molecule are not reported. (c) Zeeman diagram of the Tb ion coupled to an unpaired spin. Among the 16 intersections between the  $|J_z = +6, S_z = -1/2\rangle$  and  $|J_z = -6, S_z = +1/2\rangle$ , four are avoided level-crossings with a tunnel splitting of  $1 \mu\text{K}$ , idem for the intersections between  $|J_z = +6, S_z = -1/2\rangle$  and  $|J_z = -6, S_z = -1/2\rangle$ . (d) The experimental histogram is identical to the one presented in Figure 4a, measured at  $20 \text{ mT} \cdot \text{s}^{-1}$  sweep rate and under 0.5 T transverse field.

constant,  $\gamma$ . A dipolar interaction cannot account for the strength of the interaction since a distance of 0.1 nm between the Tb and the radical spin would be necessary in order to generate such a dipolar coupling, and the actual minimum distance between the Tb and the Pc group is  $\sim 0.5$  nm. Only an exchange-like interaction could explain a coupling of 0.4 K, but theoretical calculations would be necessary to describe in detail the overlap between the different wave functions. Nevertheless, this interpretation is supported by similar measurements done by Vincent et al. in a TbPc<sub>2</sub> transistor configuration where a Kondo ridge has been observed in transport measurements. This ridge is split in energy at zero magnetic field, see Supporting Information of ref 18, which is the signature of a strong interaction between the Pc quantum dot and the Tb ion. The interaction is estimated to be  $\sim 350$  mT, while in the present experiment it is found to be  $\sim 300$  mT.

One important parameter for potential applications in quantum information processing is the transition line width. We can see in Figure 5d that the transition line width around zero field is much broader than the one at high field. This can be explained by the presence of a spin bath surrounding the molecule. At zero field the bath is nonpolarized and acts as a small fluctuating magnetic field on both the Tb ion and the radical, while at higher magnetic field it becomes polarized and

therefore stops fluctuating. In order to measure more accurately the line width, an electron spin resonance experiment on this system would be required. Moreover, the strong coupling between the Tb electronic moment and the radical spin offers the possibility to directly entangle the latter with the Tb nuclei by using the electronuclear double resonance technique,<sup>22</sup> which would have strong potential in quantum information.

## CONCLUSION

We have quantitatively investigated the coupling between a terbium ion and a radical in a single TbPc<sub>2</sub> complex. The measurement process is achieved thanks to a molecular spin valve and a transverse field technique that allow the read-out of a single Tb ion. A detailed study of the Tb magnetization reversals offers a direct measurement of the hyperfine interaction between the electronic and nuclear magnetic moment in the Tb ion. Also, we exploit these measurements along with a numerical diagonalization of a three spins Hamiltonian to extract the exchange interaction between the radical spin located in the phthalocyanine ligands and the terbium electronic moment. Combining the electronuclear double resonance technique with the spin-valve read-out will open strong perspectives for applications in quantum information processing.

## EXPERIMENTAL SECTION

Our magnetic sensor is composed of a carbon nanotube transistor laterally coupled to the molecules through  $\pi$ - $\pi$  interactions. The carbon nanotube is grown by chemical vapor deposition on a 300 nm thick SiO<sub>2</sub> surface supported by a highly doped silicon back-gate. Nanotubes are contacted by standard e-beam lithography followed by evaporation of a 40 nm thick Pd layer, see Figure 3a. Once the device is fabricated, the surface is cleaned under Ar flow at 300 °C and a solution containing the neutral TbPc<sub>2</sub><sup>\*</sup> complexes at 10<sup>-7</sup> mol L<sup>-1</sup> is dropcasted onto the device and then dried under N<sub>2</sub> gas flow. The sample is mounted in a dilution refrigerator and cooled down to 40 mK. A 2D vectorial magnet allows to apply an inplane magnetic field up to 1.2 T.

**Conflict of Interest:** The authors declare no competing financial interest.

**Acknowledgment.** This work has been partially supported by European Community through the FET-Proactive Project MoQuaS, contract No. 610449, and the Agence Nationale de la Recherche project MolQuSpin, contract No. ANR-13-BS10. The samples were manufactured at the NANOFAB facilities of the Néel Institute. We wish to thank B. Fernandez, G. Julie, S. Dufresne, T. Crozes, and T. Fournier for their assistance in manufacturing the nanotube device. We also wish to thank F. Balestro, S. Thiele, and R. Vincent for fruitful discussions, N.-V. Nguyen and J.-P. Cleuziou for the carbon nanotube growth, and E. Bonet, C. Thirion, and R. Piquere for the software development. We also thank E. Eyraud, R. Haettel, C. Hoarau, D. Lepoittevin, and V. Reita for their technical support.

## REFERENCES AND NOTES

- Bogani, L.; Wernsdorfer, W. Molecular Spintronics Using Single-Molecule Magnets. *Nat. Mater.* **2008**, *7*, 179–186.
- Sanvito, S. Molecular Spintronics. *Chem. Soc. Rev.* **2011**, *40*, 3336–3355.
- Rocha, A. R.; García-Suárez, V. M.; Bailey, S. W.; Lambert, C. J.; Ferrer, J.; Sanvito, S. Towards Molecular Spintronics. *Nat. Mater.* **2005**, *4*, 335–339.
- Hueso, L. E.; Pruneda, J. M.; Ferrari, V.; Burnell, G.; Valdés-Herrera, J. P.; Simons, B. D.; Littlewood, P. B.; Artacho, E.; Fert, A.; Mathur, N. D. Transformation of Spin Information into Large Electrical Signals Using Carbon Nanotubes. *Nature* **2007**, *445*, 410–413.
- Ababei, R.; Pichon, C.; Roubeau, O.; Li, Y.-G.; Bréfuel, N.; Buisson, L.; Guionneau, P.; Mathonière, C.; Clérac, R. Rational Design of a Photomagnetic Chain: Bridging Single-Molecule Magnets With a Spin-Crossover Complex. *J. Am. Chem. Soc.* **2013**, *135*, 14840–14853.
- Zyazin, A. S.; van den Berg, J. W. G.; Osorio, E. A.; van der Zant, H. S. J.; Konstantinidis, N. P.; Leijnse, M.; Wegewijs, M. R.; May, F.; Hofstetter, W.; Danieli, C.; et al. Electric Field Controlled Magnetic Anisotropy in a Single Molecule. *Nano Lett.* **2010**, *10*, 3307–3311.
- Wernsdorfer, W. Molecular Nanomagnets: Towards Molecular Spintronics. *Int. J. Nanotechnol.* **2010**, *7*, 497–522.
- Ardavan, A.; Rival, O.; Morton, J.; Blundell, S.; Tyryshkin, A.; Timco, G.; Winpenny, R. Will Spin-Relaxation Times in Molecular Magnets Permit Quantum Information Processing? *Phys. Rev. Lett.* **2007**, *98*, 057201.
- Wernsdorfer, W.; Ohm, T.; Sangregorio, C.; Sessoli, R.; Mailly, D.; Paulsen, C.; Fourier, J.; Cedex, G. Observation of the Distribution of Molecular Spin States by Resonant Quantum Tunneling of the Magnetization. *Phys. Rev. Lett.* **1999**, *82*, 3903–3906.
- Wernsdorfer, W.; Sessoli, R. Quantum Phase Interference and Parity Effects in Magnetic Molecular Clusters. *Science* **1999**, *284*, 133–135.

11. Pedersen, K. S.; Bendix, J.; Clérac, R. Single-Molecule Magnet Engineering: Building-Block Approaches. *Chem. Commun.* **2014**, *50*, 4396–4415.
12. Mannini, M.; Pineider, F.; Sainctavit, P.; Danieli, C.; Otero, E.; Sciancalepore, C.; Talarico, A. M.; Arrio, M.-A.; Cornia, A.; Gatteschi, D.; et al. Magnetic Memory of a Single-Molecule Quantum Magnet Wired to a Gold Surface. *Nat. Mater.* **2009**, *8*, 194–197.
13. Ishikawa, N.; Sugita, M.; Ishikawa, T.; Koshihara, S.-Y. Mononuclear Lanthanide Complexes with a Long Magnetization Relaxation Time at High Temperatures: A New Category of Magnets at the Single-Molecular Level. *J. Phys. Chem. B* **2004**, *14*, 11265–11271.
14. Ishikawa, N.; Sugita, M.; Wernsdorfer, W. Nuclear Spin Driven Quantum Tunneling of Magnetization in a New Lanthanide Single-Molecule Magnet: Bis(phthalocyaninato)holmium Anion. *J. Am. Chem. Soc.* **2005**, *127*, 3650–3651.
15. Thiele, S.; Balestro, F.; Ballou, R.; Klyatskaya, S.; Ruben, M.; Wernsdorfer, W. Electrically Driven Nuclear Spin Resonance in Single-Molecule Magnets. *Science* **2014**, *344*, 1135–1138.
16. Glebe, U.; Weidner, T.; Baio, J. E.; Schach, D.; Bruhn, C.; Buchholz, A.; Plass, W.; Walleck, S.; Glaser, T.; Siemeling, U. Self-Assembled Monolayers of Single-Molecule Magnets [Tb(Pc'(SR)<sub>8</sub>)<sub>2</sub>] on Gold. *ChemPlusChem* **2012**, *77*, 889–897.
17. Katoh, K.; Yoshida, Y.; Yamashita, M.; Miyasaka, H.; Breedlove, B. K.; Kajiwara, T.; Takaishi, S.; Ishikawa, N.; Isshiki, H.; Zhang, Y. F.; et al. Direct Observation of Lanthanide(III)-Phthalocyanine Molecules on Au(111) by Using Scanning Tunneling Microscopy and Scanning Tunneling Spectroscopy and Thin-Film Field-Effect Transistor Properties of Tb(III)- and Dy(III)-Phthalocyanine Molecules. *J. Am. Chem. Soc.* **2009**, *131*, 9967–9976.
18. Vincent, R.; Klyatskaya, S.; Ruben, M.; Wernsdorfer, W.; Balestro, F. Electronic Read-Out of a Single Nuclear Spin Using a Molecular Spin Transistor. *Nature* **2012**, *488*, 357–360.
19. Lopes, M.; Candini, A.; Urdampilleta, M.; Reserbat-Plantey, A.; Bellini, V.; Klyatskaya, S.; Marty, L.; Ruben, M.; Affronte, M.; Wernsdorfer, W.; et al. Surface-Enhanced Raman Signal for Terbium Single-Molecule Magnets Grafted on Graphene. *ACS Nano* **2010**, *4*, 7531–7537.
20. Klyatskaya, S.; Mascarós, J. R. G.; Bogani, L.; Hennrich, F.; Kappes, M.; Wernsdorfer, W.; Ruben, M. Anchoring of Rare-Earth-Based Single-Molecule Magnets on Single-Walled Carbon Nanotubes. *J. Am. Chem. Soc.* **2009**, *131*, 15143–15151.
21. Ishikawa, N.; Sugita, M.; Tanaka, N.; Ishikawa, T.; Koshihara, S.-y.; Kaizu, Y. Upward Temperature Shift of the Intrinsic Phase Lag of the Magnetization of Bis(phthalocyaninato) terbium by Ligand Oxidation Creating an  $S = 1/2$  Spin. *Inorg. Chem.* **2004**, *43*, 5498–5500.
22. Simmons, S.; Brown, R. M.; Riemann, H.; Abrosimov, N. V.; Becker, P.; Pohl, H.-J.; Thewalt, M. L. W.; Itoh, K. M.; Morton, J. J. L. Entanglement in a Solid-State Spin Ensemble. *Nature* **2011**, *470*, 69–72.
23. Katoh, K.; Kajiwara, T.; Nakano, M.; Nakazawa, Y.; Wernsdorfer, W.; Ishikawa, N.; Breedlove, B. K.; Yamashita, M. Magnetic Relaxation of Single-Molecule Magnets in an External Magnetic Field: an Ising Dimer of a Terbium(III)-Phthalocyaninate Triple-Decker Complex. *Chem.—Eur. J.* **2011**, *17*, 117–122.
24. Komeda, T.; Isshiki, H.; Liu, J.; Zhang, Y.-F.; Lorente, N.; Katoh, K.; Breedlove, B. K.; Yamashita, M. Observation and Electric Current Control of a Local Spin in a Single-Molecule Magnet. *Nat. Commun.* **2011**, *2*, 217–224.
25. Ofelt, G. S. Structure of the  $f_6$  Configuration with Application to Rare-Earth Ions. *J. Chem. Phys.* **1963**, *38*, 2171–2180.
26. Ishikawa, N.; Sugita, M.; Okubo, T.; Tanaka, N.; Iino, T.; Kaizu, Y. Determination of Ligand-Field Parameters and  $f$ -Electronic Structures of Double-Decker Bis(phthalocyaninato)lanthanide Complexes. *Inorg. Chem.* **2003**, *42*, 2440–2446.
27. Wernsdorfer, W.; Bhaduri, S.; Vinslava, A.; Christou, G. Landau-Zener Tunneling in the Presence of Weak Intermolecular Interactions in a Crystal of Mn<sub>4</sub> Single-Molecule Magnets. *Phys. Rev. B* **2005**, *72*, 214429.
28. Wernsdorfer, W. From Micro- to Nano-SQUIDS: Applications to Nanomagnetism. *Supercond. Sci. Technol.* **2009**, *22*, 064013.
29. Branzoli, F.; Carretta, P.; Filibian, M.; Klyatskaya, S.; Ruben, M. Low-Energy Spin Dynamics in the [YPC<sub>2</sub>]<sup>0</sup>  $S = 1/2$  Antiferromagnetic Chain. *Phys. Rev. B* **2011**, *83*, 174419.
30. Urdampilleta, M.; Klyatskaya, S.; Cleuziou, J.-P.; Ruben, M.; Wernsdorfer, W. Supramolecular Spin Valves. *Nat. Mater.* **2011**, *10*, 502–506.
31. Urdampilleta, M.; Nguyen, N.-V.; Cleuziou, J.-P.; Klyatskaya, S.; Ruben, M.; Wernsdorfer, W. Molecular Quantum Spintronics: Supramolecular Spin Valves Based on Single-Molecule Magnets and Carbon Nanotubes. *Int. J. Mol. Sci.* **2011**, *12*, 6656–6667.
32. Urdampilleta, M.; Klyatskaya, S.; Ruben, M.; Wernsdorfer, W. Landau-Zener Tunneling of a Single Tb<sup>3+</sup> Magnetic Moment Allowing the Electronic Read-Out of a Nuclear Spin. *Phys. Rev. B* **2013**, *87*, 195412.
33. Ganzhorn, M.; Klyatskaya, S.; Ruben, M.; Wernsdorfer, W. Strong Spin-Phonon Coupling Between a Single-Molecule Magnet and a Carbon Nanotube Nanoelectromechanical System. *Nat. Nanotechnol.* **2013**, *8*, 165–169.